Monte Carlo Methods Appl. Vol. 14 No. 4 (2008), pp. 311–329
DOI 10.1515 / MCMA.2008.014

Realizability of dynamic subgrid-scale stress models via stochastic analysis

Stefan Heinz

Abstract. Large eddy simulations involving dynamic subgrid-scale stress models reveal questions regarding the formulation of dynamic stress models. The dynamic Smagorinsky model, for example, yields large fluctuations and can easily become unstable. An analysis explains the reasons for these problems: it is shown that the dynamic Smagorinsky model involves an incorrect scale dependence which may produce significant errors leading to instabilities. These problems are addressed by analyzing the implications of the realizability constraint, this means the constraint that an acceptable turbulence closure model be based on the statistics of a velocity field that is physically achievable or realizable. The realizable dynamic stress models obtained have strong theoretical support: these models are the result of a well based systematic development of stress models. From a practical point of view, the realizable dynamic stress models obtained have the advantage that they do not support the development of instabilities due to possibly huge model errors. It is also shown that the consideration of nonlinear dynamic stress models further improves the accuracy of simulations.

Keywords. Large eddy simulation, Monte Carlo methods, stochastic subgrid-scale modeling, dynamic subgrid-scale models, nonlinear subgrid-scale models.

1. Introduction

Large eddy simulation (LES) represents a very promising alternative to other methods for the computation of turbulent flows [5, 21, 28, 33, 37, 40]. On the one hand, LES is computationally much more efficient than direct numerical simulation (DNS) because not all the spectrum of turbulent motions has to be resolved. On the other hand, LES has more predictive power than Reynolds-averaged Navier–Stokes (RANS) methods because the most energetic turbulence structures are described without modeling assumptions. The closure of LES equations requires, however, modeling assumptions for small-scale processes. Research over forty years revealed that such subgrid-scale (SGS) modeling represents a non-trivial problem: many different SGS models are currently in use, and the evaluation of various models represents a dominant research activity [5, 21, 28, 33, 37, 40]. The latter fact reveals the need for thorough analysis of mathematical and physical constraints on the modeling of SGS processes [4, 7].

An important guiding principle for such mathematical analysis is given by the realizability constraint [25, 41, 46]. The realizability requirement enunciates the rudimentary expectation that an acceptable turbulence closure model be based on the

statistics of a velocity field that is physically achievable or realizable. For example, the Reynolds stress tensor (i.e. the correlation of velocity fluctuations) of any velocity field governed by the Navier–Stokes equations is positive semi-definite. The latter property implies that the Reynolds stress has non-negative diagonal components (energies), off-diagonal components that satisfy the Schwarz inequality, and a non-negative determinant (which implies an additional condition on cross-correlations). In correspondence to these properties of the Reynolds stress, the realizability constraint as proposed by Schumann requires that the modeled Reynolds stress also has to be positive semi-definite [41]. Over the last three decades, the Schumann realizability constraint has served as the theoretical basis for several refined realizability concepts [2, 9, 35, 36, 45, 51]. The use of realizable turbulence closure models was found to be of remarkable relevance to applications [17, 30, 39, 44]. The Schumann realizability constraint can be also adopted for the development of realizable SGS stress tensor models [4, 7, 47] provided that the filter function is positive [47].

However, the Reynolds stress tensor is the result of a variety of processes such that Reynolds stress models may be very complex. The latter fact can make it difficult or even impossible to ensure the realizability of stress models [1, 2, 36, 37, 45, 51]. This problem can be solved by the following approach. The Reynolds stress represents the variance of the probability density function (PDF) of turbulent velocities. The realizability of the Reynolds stress can be ensured, therefore, by the realizability of the PDF of turbulent velocities. The latter can be achieved by a physically realizable stochastic model for turbulent velocities [2, 35, 36, 45] which determines a transport equation for the PDF of turbulent velocities. The velocity PDF transport equation can be used for the derivation of realizable transport equations for the stress tensor and the derivation of simpler algebraic stress models [1, 3, 12, 37]. Another option is to solve the PDF transport equation by Monte Carlo simulation. In this way, the Reynolds stress can be calculated without adopting additional assumptions. The benefits of such realizable methods were proved in several applications of PDF methods [31, 32, 50]. Basically the same approach can be applied to develop stochastic velocity models which generalize LES equations [8, 10, 11, 12, 34, 38, 42, 43]. The latter models determine a transport equation for the filter density function (FDF), which represents the PDF with regard to the LES approach. As shown recently, such FDF models can be used for the development of realizable linear and nonlinear SGS stress models [11, 12, 14, 15].

A well-known limitation of SGS stress models is given by the use of constant model parameters (like the Smagorinsky coefficient). The use of constant model parameters turned out to be inappropriate to accurately calculate, for example, laminar flows, transitional flows and near-wall regions [28, 37, 40]. Thus, with regard to every application there is the question of which model parameters are appropriate for the flow considered. A solution for this problem was pioneered by Germano who introduced the idea of dynamic SGS stress models [6, 23, 29]. However, the dynamic calculation of model parameters proposed by Germano is only one possible choice, and applications reveal

several questions regarding the suitability of the current way to formulate dynamic SGS stress models [18, 19, 26].

To address these questions, the formulation of dynamic SGS stress models will be considered here on the basis of the stochastic modeling approach for the derivation of realizable equations for the dynamics of SGS velocities. The paper is organized in the following way. Sections 2 and 3 describe the dynamic Smagorinsky model and deal with an analysis of its problems, respectively. Section 4 explains how the stochastic modeling approach can be used for the derivation of realizable linear and nonlinear SGS stress models. On this basis, realizable dynamic SGS stress models will be derived in Section 5. Section 6 deals with a comparison with corresponding other SGS stress models, and Section 7 summarizes the conclusions of this analysis.

2. The dynamic Smagorinsky model

To justify the requirement to address the formulation of dynamic stress models, let us consider the problems of currently used methods to provide the coefficients in SGS stress models. The Smagorinsky model $\tau_{ij}^d = -2\nu_t \widetilde{S}_{ij}^d$ represents the most popular model for the SGS stress tensor [28, 37, 40]. τ_{ij}^d represents the deviatoric part of the SGS stress tensor $\tau_{ij} = \tau_{kk}\delta_{ij}/3 + \tau_{ij}^d$. Here, δ_{ij} refers to the Kronecker symbol, and $\tau_{kk} = 2k$, where k refers to the residual turbulent kinetic energy. The sum convention is used throughout this paper for repeated subscripts. The deviatoric stress τ_{ij}^d is assumed to be proportional to the deviatoric part $\widetilde{S}_{ij}^d = \widetilde{S}_{ij} - \widetilde{S}_{nn}\delta_{ij}/3$ of the resolved rate-of-strain tensor $\widetilde{S}_{ij}$. The stress model is unclosed as long as the SGS viscosity ν_t is not specified. According to the Smagorinsky model, this viscosity is parameterized by $\nu_t = c_S\Delta^2|\widetilde{S}^d|$. Here, c_S is the Smagorinsky coefficient, Δ is the filter width, and $|\widetilde{S}^d| = (2\widetilde{S}_{kl}^d\widetilde{S}_{lk}^d)^{1/2}$ is the characteristic strain rate.

The Smagorinsky coefficient c_S is often considered to be constant. However, the use of a constant Smagorinsky coefficient c_S turned out to be inappropriate to accurately calculate, for example, laminar flows, transitional flows and near-wall regions [28, 37, 40]. A solution for this problem was pioneered by Germano who introduced the idea of dynamic SGS stress models [6, 23, 29]. Germano's approach is based on the identity $L_{ij} = T_{ij} - \overline{\tau}_{ij}$, which relates the test-filtered SGS stress $\overline{\tau}_{ij}$ to the subtest-scale (STS) stress T_{ij} and the known resolved stress tensor L_{ij}. Written for the deviatoric components, Germano's identity reads $L_{ij}^d = T_{ij}^d - \overline{\tau}_{ij}^d$. In correspondence to the Smagorinsky model, one may assume a similar expression $T_{ij}^d = -2\nu_t^T\,\overline{\widetilde{S}}_{ij}^{\,d}$ for the deviatoric STS stress. Here, $\overline{\widetilde{S}}_{ij}^{\,d}$ is the test-scale deviatoric strain tensor and $\nu_t^T = c_S(\Delta^T)^2\,|\overline{\widetilde{S}}^{\,d}|$ refers to the STS viscosity, where Δ^T and $|\overline{\widetilde{S}}^{\,d}| = (2\overline{\widetilde{S}}_{kl}^{\,d}\overline{\widetilde{S}}_{lk}^{\,d})^{1/2}$ are the test filter width and test-scale characteristic strain rate, respectively. The assumption

for T_{ij}^d applied allows the rewriting

$$L_{ij}^d = -c_S H_{ij} \tag{1}$$

of Germano's identity, where H_{ij} is given by

$$H_{ij} = 2\left(\Delta^T\right)^2 |\overline{\widetilde{S}}^d| \, \overline{\widetilde{S}}_{ij}^d - 2\Delta^2 \, \overline{|\widetilde{S}^d| \, \widetilde{S}_{ij}^d}. \tag{2}$$

Expression (1) provides five conditions for c_S in terms of the known L_{ij}^d and H_{ij}. A simple way to use these conditions for the calculation of c_S is to multiply (1) with H_{ij}. In this way, c_S is given by

$$c_S = -\frac{L_{ij}^d H_{ji}}{H_{mn} H_{nm}}. \tag{3}$$

The calculation of c_S by expression (3) cannot satisfy all the five conditions for c_S provided by (1), which implies an error $E_{ij} = L_{ij}^d + c_S H_{ij}$ related to the use of (3). However, it is relevant to note that expression (3) minimizes the squared error $E_{ij}E_{ji}$ [23]. The use of $\nu_t = c_S \Delta^2 \, |\widetilde{S}^d|$ applied in conjunction with expression (3) for the calculation of c_S will be referred to below as dynamic Smagorinsky model (DSM).

The error analysis is known to represent a valuable tool for investigations of the performance of dynamic SGS models [27]. To prepare the analysis of errors related to several SGS stress models in the following sections, it is helpful to introduce according to the definition of $|\widetilde{S}^d|$ the characteristic magnitude of any matrix A_{ij} by

$$|A| = \sqrt{2 A_{ij} A_{ji}}. \tag{4}$$

In addition to the definition (4), we introduce for any symmetric deviatoric matrices A_{ij} and B_{ij} the abbreviation

$$r_{AB} = \frac{A_{ij} B_{ji}}{\sqrt{A_{kl} A_{lk} B_{mn} B_{nm}}}. \tag{5}$$

By following the derivation of properties of correlation coefficients [12], one can show that r_{AB} has the property $-1 \leq r_{AB} \leq 1$ of a correlation coefficient. By adopting the definitions (4) and (5), expression (3) for c_S and the standardized error $e_S = |E|^2/|L^d|^2$ related to the DSM can be written

$$c_S = -r_{LH} \frac{|L^d|}{|H|}, \qquad e_S = 1 - {r_{LH}}^2. \tag{6}$$

The degree of correlation between L_{ij}^d and H_{ij} determines, therefore, the standardized error e_S related to the DSM.

3. Some questions related to the dynamic Smagorinsky model

It is worth noting that expression (1) for L_{ij}^d is not the only possible choice for L_{ij}^d [18, 19], and there are indications that the current use of the dynamic procedure does not represent an optimal formulation. The DSM yields large fluctuations and can easily become unstable. Applying averaging in homogeneous directions to obtain the Smagorinsky constant (or the use of empirical clipping procedures) eliminates the stability problem but the model loses generality and the ability to account for backscatter [18, 19, 26].

To see the features of the DSM in more detail, it is helpful to rewrite H_{ij} in the following way,

$$H_{ij} = 2\left(\Delta^T\right)^2 |\overline{\widetilde{S}}^d| \left\{ \overline{\widetilde{S}}^d_{ij} - r^2 R_{ij} \right\}, \tag{7}$$

where the abbreviations $R_{ij} = \overline{|\widetilde{S}^d| \widetilde{S}^d_{ij}} / |\overline{\widetilde{S}}^d|$ and $r = \Delta/\Delta^T$ are introduced. The Smagorinsky coefficient c_S and the standardized error $e_S = |E|^2/|L^d|^2$ related to the DSM are then given by

$$c_S = -\frac{\alpha}{2} \frac{1}{1-\gamma r^2} \frac{r_{LS} - \Delta_{LR}}{1 - \Delta_{SR}}, \qquad e_S = 1 - \frac{\left(r_{LS} - \Delta_{LR}\right)^2}{1 - \Delta_{SR}}. \tag{8}$$

In these expressions, $\alpha = |L^d|/(\Delta^T |\overline{\widetilde{S}}^d|)^2$, $\gamma = |R|/|\overline{\widetilde{S}}^d|$, and Δ_{LR} and Δ_{SR} are given by

$$\Delta_{LR} = \left(r_{LR} - r_{LS}\right) \frac{\gamma r^2}{1-\gamma r^2}, \qquad \Delta_{SR} = 2\left(r_{SR} - 1\right) \frac{\gamma r^2}{\left(1-\gamma r^2\right)^2}. \tag{9}$$

Here, r_{LS}, r_{LR}, and r_{SR} are defined according to (5). With regard to r_{LS} and r_{SR}, it is worth noting that the subscript S refers to the use of the deviatoric test-scale shear matrix $\overline{\widetilde{S}}^d_{ij}$.

Essential features of the DSM may be seen by adopting the reasonable approximation $\overline{|\widetilde{S}^d| \widetilde{S}^d_{ij}} \approx |\overline{\widetilde{S}}^d| \overline{\widetilde{S}}^d_{ij}$ (which means $R_{ij} = \overline{\widetilde{S}}^d_{ij}$). In this case, $\gamma = 1$ and (because of $r_{LR} = r_{LS}$ and $r_{SR} = 1$) we find that $\Delta_{LR} = \Delta_{SR} = 0$. Hence, relations (8) simplify to $c_S = -0.5\alpha r_{LS}/(1-r^2)$ and $e_S = 1 - {r_{LS}}^2$. The variation of c_S with $r = \Delta/\Delta^T$ describes a transition from $c_S(r=0)$ to $c_S(r=1)$. The parametrization $\nu_t^T = c_S(\Delta^T)^2 |\overline{\widetilde{S}}^d|$ applied suggests a r value relatively close to 1: otherwise it is unclear whether c_S can be considered to be unaffected by the test scale. However, c_S does not exist for $r \to 1$ which represents an unphysical behavior. The fact that c_S does not exist for $r \to 1$ can also be seen by considering the model assumption $L_{ij}^d = -c_S H_{ij}$ directly. A finite L_{ij}^d implies $c_S \to \infty$ because H_{ij} vanishes for $R_{ij} = \overline{\widetilde{S}}^d_{ij}$ and $r \to 1$, see expression (7). The latter observation supports the view that the variation of c_S with r is incorrect. Apart from that, the parameter r is unknown. Thus, the DSM specification of c_S has an empirical character, and a scale dependence of c_S implies grid-dependent solutions.

In general, R_{ij} will be unequal to $\overline{\widetilde{S}}^{\,d}_{ij}$. For this case, expression (8) shows that c_S and e_S can be affected by nonzero Δ_{SR} and Δ_{LR}. The definition of Δ_{SR} implies that $\Delta_{SR} \leq 0$. Therefore, Δ_{SR} increases the error e_S, and this effect grows with r because Δ_{SR} increases with r. Δ_{LR} represents a fluctuating variable: Δ_{LR} may be positive or negative depending on the sign of $r_{LR} - r_{LS}$. The variance of Δ_{LR} increases with r because the magnitude of Δ_{LR} increases with r. The appearance of such fluctuations may imply significant errors. A more detailed analysis of the features of the DSM will be provided in Section 6 in comparison to other SGS stress models.

4. Realizable SGS stress models

The discussion of shortcomings of the DSM in the previous section reveals the need to reconsider the formulation of dynamic SGS stress models. The latter question will be addressed on the basis of realizable stochastic equations for the dynamics of SGS velocities. In this section, it will be shown how it is possible to use the stochastic velocity equations for the derivation of linear and nonlinear SGS stress models. On this basis, corresponding dynamic stress models will be derived in Section 5.

The SGS stress models considered below are based on the fundamental equations for the instantaneous fluid mass density $\rho(\boldsymbol{x},t)$ and velocity $U_i(\boldsymbol{x},t)$, where $i = 1,3$. These equations read

$$\frac{\partial \rho}{\partial t} + \frac{\partial \rho U_k}{\partial x_k} = 0, \tag{10}$$

$$\frac{\partial \rho U_i}{\partial t} + \frac{\partial \rho U_k U_i}{\partial x_k} = -\frac{\partial \rho M_{ki}}{\partial x_k}. \tag{11}$$

The molecular stress tensor M_{ki} represents the variance of molecular velocity fluctuations. M_{ki} is given in the first-order approximation by the Navier–Stokes model $M_{ki} = p\delta_{ki}/\rho - 2\nu S^d_{ki}$ [13]. Here, p is the pressure and ν is the molecular viscosity. $S^d_{ij} = S_{ij} - S_{nn}\delta_{ij}/3$ refers to the deviatoric part of the rate-of-strain tensor $S_{ij} = (\partial U_i/\partial x_j + \partial U_j/\partial x_i)/2$.

The numerical solution of the equations (10) and (11) is infeasible for most flows of practical relevance because of the huge cost related to such DNS [37]. Thus, (10) and (11) have to be used for the construction of equations for filtered variables. Mass density-weighted spatially filtered variables are defined by

$$\widetilde{Q}(\boldsymbol{x},t) = \frac{\langle \rho(\boldsymbol{x},t) Q(\boldsymbol{x},t) \rangle_G}{\rho_G(\boldsymbol{x},t)}. \tag{12}$$

With regard to any function $q(\boldsymbol{x},t)$, the spatially filtered variable $\langle q(\boldsymbol{x},t)\rangle_G$ is defined here by

$$\langle q(\boldsymbol{x},t)\rangle_G = \int d\boldsymbol{r}\, q(\boldsymbol{x}+\boldsymbol{r},t) G(\boldsymbol{r}). \tag{13}$$

The filtered fluid mass density is written $\langle q(\boldsymbol{x},t)\rangle_G = \rho_G(\boldsymbol{x},t)$. The filter function G is assumed to be homogeneous, i.e., independent of $\boldsymbol{x}$. We assume $\int d\boldsymbol{r}\, G(\boldsymbol{r}) = 1$ and $G(\boldsymbol{r}) = G(-\boldsymbol{r})$. Moreover, only positive filter functions are considered for which all the moments $\int d\boldsymbol{r}\, r^m G(\boldsymbol{r})$ exist for $m \geq 0$. Thus, G has the properties of a PDF. The scale of filtering is defined by the filter width Δ which is chosen such that $\Delta \ll L$, where L is the characteristic length scale of large-scale turbulent eddies. By introducing the SGS stress tensor

$$\tau_{ki} = \widetilde{U_k U_i} - \widetilde{U}_k \widetilde{U}_i, \tag{14}$$

the equations for the filtered mass density ρ_G and velocity $\widetilde{U}_i$ can be written

$$\frac{\partial \rho_G}{\partial t} + \frac{\partial \rho_G \widetilde{U}_k}{\partial x_k} = 0, \tag{15}$$

$$\frac{\partial \rho_G \widetilde{U}_i}{\partial t} + \frac{\partial \rho_G \widetilde{U}_k \widetilde{U}_i}{\partial x_k} + \frac{\partial \rho_G\, \tau_{ki}}{\partial x_k} = -\frac{\partial \rho_G\, \widetilde{M}_{ki}}{\partial x_k}. \tag{16}$$

The problem related to the use of (15) and (16) is given by the unclosed SGS stress τ_{ki}. The stress τ_{ki} represents the variance of SGS velocity fluctuations. Thus, a way to calculate τ_{ki} is given by the development of a stochastic model for SGS fluctuations. Such a realizable stochastic velocity model is given by [11, 12, 14, 15]

$$\frac{dx_i^*}{dt} = U_i^*, \tag{17}$$

$$\frac{dU_i^*}{dt} = -\frac{1}{\rho_G}\frac{\partial \rho_G\, \widetilde{M}_{ki}}{\partial x_k} - \frac{1}{\tau_L}\left(U_i^* - \widetilde{U}_i\right) + \sqrt{\frac{4c_0 k}{3\tau_L}}\frac{dW_i}{dt}. \tag{18}$$

Here, $x_i^*(t)$ and $U_i^*(t)$ represent the ith components of a fluid particle position and velocity, and d/dt refers to the derivative by time t. The first term on the right-hand side of (18) represents filtered molecular transport. The additional two terms represent models for the relaxation and generation of SGS velocity fluctuations, respectively. The second term describes a relaxation towards the filtered velocity $\widetilde{U}_i$ with a characteristic relaxation time scale τ_L. The generation of fluctuations is described by the noise term (the last term) which is determined by the properties of dW_i/dt. The latter is a Gaussian process with vanishing means, $\langle dW_i/dt\rangle = 0$, and uncorrelated values at different times, $\langle dW_i/dt(t)\cdot dW_j/dt'(t')\rangle = \delta_{ij}\delta(t-t')$, where $\delta(t-t')$ refers to the delta function. $k = \tau_{nn}/2$ is the residual turbulent kinetic energy. The nondimensional parameter c_0 controls the noise strength. This parameter is related to the Kolmogorov constant C_0 by $c_0 = C_0/[C_0 + 2/3]$. An analysis of implications of (17) and (18) reveals that $c_0 = 19/27 \approx 0.7$ [11, 12, 14, 15].

The model (17) and (18) determines a transport equation for the FDF $F(\boldsymbol{w},\boldsymbol{x},t)$ of filtered velocities, where $\boldsymbol{w} = (w_1, w_2, w_3)$ refers to the sample space velocity. The

velocity FDF equation implied by (17) and (18) reads [12, 15]

$$\frac{\partial \rho_G F}{\partial t} + \frac{\partial w_i \rho_G F}{\partial x_i} = \frac{\partial}{\partial w_i}\left[\frac{1}{\rho_G}\frac{\partial \rho_G \widetilde{M_{ki}}}{\partial x_k} + \frac{1}{\tau_L}\left(w_i - \widetilde{U}_i\right)\right]\rho_G F + \frac{2c_0 k}{3\tau_L}\frac{\partial^2 \rho_G F}{\partial w_i \partial w_i}. \tag{19}$$

By multiplying equation (19) with 1 and w_i, respectively, and integrating over the velocity space, one finds that the stochastic model (17) and (18) reproduces exactly the equations (15) and (16) for the filtered mass density ρ_G and filtered velocity $\widetilde{U}_i$. By multiplying equation (19) with $w_i w_j$ and integrating over the velocity space, one can derive a transport equation for the SGS stress τ_{ij},

$$\frac{\widetilde{D}\tau_{ij}}{\widetilde{D}t} + \frac{1}{\rho_G}\frac{\partial \rho_G T_{kij}}{\partial x_k} + \tau_{ik}\frac{\partial \widetilde{U}_j}{\partial x_k} + \tau_{jk}\frac{\partial \widetilde{U}_i}{\partial x_k} = -\frac{2}{\tau_L}\left(\tau_{ij} - \frac{2}{3}c_0 k \delta_{ij}\right), \tag{20}$$

where $\widetilde{D}/\widetilde{D}t = \partial/\partial t + \widetilde{U}_k \partial/\partial x_k$ refers to the filtered Lagrangian time derivative, and T_{kij} refers to the triple correlation tensor of SGS velocity fluctuations. Equation (20) for the SGS stress tensor $\tau_{ij} = 2k(\delta_{ij}/3 + d_{ij})$ can be rewritten in terms of equations for the residual turbulent kinetic energy $k = \tau_{kk}/2$ and standardized anisotropy tensor $d_{ij} = (\tau_{ij} - 2k\delta_{ij}/3)/2k$,

$$\frac{\widetilde{D}k}{\widetilde{D}t} + \frac{1}{2\rho_G}\frac{\partial \rho_G T_{knn}}{\partial x_k} + 2k\left(d_{kn} + \frac{1}{3}\delta_{kn}\right)\frac{\partial \widetilde{U}_n}{\partial x_k} = -\frac{2(1-c_0)k}{\tau_L}, \tag{21}$$

$$\frac{\widetilde{D}d_{ij}}{\widetilde{D}t} + \frac{1}{2\rho_G k}\frac{\partial \rho_G \left(T_{kij} - T_{knn}\delta_{ij}/3\right)}{\partial x_k} + \frac{d_{ij}}{k}\frac{\widetilde{D}k}{\widetilde{D}t} + d_{ik}\frac{\partial \widetilde{U}_j}{\partial x_k} + d_{jk}\frac{\partial \widetilde{U}_i}{\partial x_k} - \frac{2}{3}d_{kn}\frac{\partial \widetilde{U}_n}{\partial x_k}\delta_{ij} = -\frac{2}{\tau_L}d_{ij} - \frac{2}{3}\widetilde{S}^d_{ij}. \tag{22}$$

Equations (21) and (22) can be closed by specifying a model for T_{kij} [12]. A computationally less expensive way is given by the use of an algebraic SGS stress model. The first-order approximation for the anisotropy tensor d_{ij} is given by the balance of the terms on the right-hand side of equation (22), this means $d_{ij}{}^{(1)} = -\widetilde{S}^d_{ij}\tau_L/3$. The latter result implies in the first order of approximation for the deviatoric SGS stress tensor $\tau^d_{ij} = \tau_{ij} - 2k\delta_{ij}/3$ the expression

$$\tau^{d\,(1)}_{ij} = -2\nu_t \widetilde{S}^d_{ij}, \tag{23}$$

where the SGS viscosity $\nu_t = k\tau_L/3$ is introduced. The second order of approximation for d_{ij} is given by using the usual assumption that the first three terms on the left-hand side of (22) are negligibly small. By adopting the first-order approximation for d_{ij} in

all the other expressions on the left-hand side of (22), we find the following second order of approximation

$$\tau_{ij}^{d\,(2)} = -2\nu_t\,\widetilde{S}_{ij}^d - \nu_t\tau_L\left[\widetilde{S}_{ik}^d\widetilde{\Omega}_{kj} + \widetilde{S}_{jk}^d\widetilde{\Omega}_{ki} - 2\widetilde{S}_{ik}^d\widetilde{S}_{kj}^d + \frac{2}{3}\widetilde{S}_{nk}^d\widetilde{S}_{kn}^d\delta_{ij}\right]. \qquad (24)$$

Here, $\widetilde{\Omega}_{ij} = (\partial\widetilde{U}_i/\partial x_j - \partial\widetilde{U_j}/\partial x_i)/2$ represents the resolved rate-of-rotation tensor. The relevance of nonlinear stress contributions for complex flow simulations is known (the assumption of a linear relationship between the SGS stress and resolved strain tensors is clearly questionable for such flows) [12, 14, 15, 16, 20, 48, 49]. In contrast to nonlinear SGS stress models provided by other approaches [16, 20, 48, 49], it is worth emphasizing that all the coefficients in expression (24) are determined by the parameters of the stochastic model (17) and (18).

The stochastic model (17) and (18) and its implied SGS stress models are unclosed as long as the relaxation time scale τ_L is not defined. An analysis of the τ_L scaling reveals that $\tau_L = \ell_*\Delta k^{-1/2}$, where $\ell_* = (1 \pm 0.5)/3$ [11]. By adopting this relation for τ_L, the SGS viscosity can be written $\nu_t = c_K\nu_K$, where $c_K = \ell_*/3$ and $\nu_K = \Delta k^{1/2}$. This parametrization for ν_t was used in several applications [22, 37]. To use $\nu_t = c_K\nu_K$, one has to solve (21) to obtain the residual turbulent kinetic energy k. A way to overcome this problem is to assume a balance between the production and dissipation in equation (21) given by $d_{kn}\,^{(1)}\partial\widetilde{U}_k/\partial x_n\,\tau_L = c_0 - 1$. By adopting $d_{ij}\,^{(1)} = -\widetilde{S}_{ij}^d\tau_L/3$ and $c_0 = 19/27$, one finds in this way $|\widetilde{S}^d|\,\tau_L = 4/3$. Combined with $\tau_L = \ell_*\Delta k^{-1/2}$, the latter expression provides an equilibrium value $k_e^{1/2} = 3\ell_*\Delta|\widetilde{S}^d|/4$ for $k^{1/2}$. The corresponding equilibrium SGS viscosity is given by $\nu_t = c_S\nu_S$, where $c_S = (\ell_*/2)^2$ and $\nu_S = \Delta^2|\widetilde{S}^d|$. It is worth noting that the use of $\ell_* = 1/3$ recovers the standard value $c_S = (1/6)^2$ for the Smagorinsky coefficient [22, 37].

By adopting the expressions for the SGS viscosity ν_t obtained above, the second order of approximation (24) for the deviatoric SGS stress tensor τ_{ij}^d can be written

$$\tau_{ij}^d = -2c_*\nu_*\,\widetilde{S}_{ij}^d - c_N\Delta^2\left[\widetilde{S}_{ik}^d\widetilde{\Omega}_{kj} + \widetilde{S}_{jk}^d\widetilde{\Omega}_{ki} - 2\widetilde{S}_{ik}^d\widetilde{S}_{kj}^d + \frac{2}{3}\widetilde{S}_{nk}^d\widetilde{S}_{kn}^d\delta_{ij}\right]. \qquad (25)$$

To generalize the ν_t parameterizations described above, the SGS viscosity is written $\nu_t = c_*\nu_*$ in expression (25). Here, $c_*\nu_*$ can be given either by the non-equilibrium model $c_K\nu_K$, or $c_*\nu_*$ can be given by the equilibrium model $c_S\nu_S$, this means

$$c_*\nu_* = \left\{\begin{array}{lll} c_K\nu_K: & c_K = \ell_*/3; & \nu_K = \Delta\,k^{1/2} \\ c_S\nu_S: & c_S = (\ell_*/2)^2; & \nu_S = \Delta^2\,|\widetilde{S}^d| \end{array}\right\}. \qquad (26)$$

The parameter c_N in (25) is given by $c_N = \ell_*^2/3$. The first-order approximation for τ_{ij}^d can be recovered by setting $c_N = 0$.

5. Realizable dynamic SGS stress models

The closure of expression (25) for the SGS stress τ_{ij}^d requires the determination of the coefficients c_* and c_N. For doing this, we follow the idea of the dynamic modeling approach. First, the filtered equations (15) and (16) will be filtered again by adopting another filter (the test filter). Second, the resulting test-filtered equations will be closed in equivalence to the closure of the filtered equations (15) and (16). This approach gives the opportunity to relate c_* and c_N to quantities that are known.

To derive the test-filtered equations, we define the test filter operation by

$$\overline{Q}(\boldsymbol{x},t) = \frac{\langle \rho_G(\boldsymbol{x},t) Q(\boldsymbol{x},t) \rangle_T}{\rho_{GT}(\boldsymbol{x},t)}. \tag{27}$$

With regard to any function $q(\boldsymbol{x},t)$, the test-filtered variable $\langle q(\boldsymbol{x},t)\rangle_T$ is defined here by

$$\langle q(\boldsymbol{x},t)\rangle_T = \int d\boldsymbol{r} q(\boldsymbol{x}+\boldsymbol{r},t) T(\boldsymbol{r}). \tag{28}$$

The difference to the definition (13) for a spatially filtered variable $\langle q(\boldsymbol{x},t)\rangle_G$ is given by the fact that the test filter function T is used here instead of the filter function G in expression (13). The test-filtered $\rho_G(\boldsymbol{x},t)$ is given by $\langle \rho_G(\boldsymbol{x},t)\rangle_T = \rho_{GT}(\boldsymbol{x},t)$. In correspondence to the definition (14) of the SGS stress tensor, the STS stress T_{ki} is defined by

$$T_{ki} = \widetilde{\overline{U_k U_i}} - \overline{\widetilde{U}}_k \overline{\widetilde{U}}_i. \tag{29}$$

An exact relation between the STS stress T_{ki} and the SGS stress τ_{ki} is given by Germano's identity $L_{ij} = T_{ij} - \overline{\tau}_{ij}$, where $L_{ki} = \overline{\widetilde{U}_k \widetilde{U}_i} - \overline{\widetilde{U}}_k \overline{\widetilde{U}}_i$ refers to the resolved stress (which is known). By adopting $L_{ij} = T_{ij} - \overline{\tau}_{ij}$, one finds for the test-filtered mass density and velocities the equations

$$\frac{\partial \rho_{GT}}{\partial t} + \frac{\partial \rho_{GT} \overline{\widetilde{U}}_k}{\partial x_k} = 0, \tag{30}$$

$$\frac{\partial \rho_{GT} \overline{\widetilde{U}}_i}{\partial t} + \frac{\partial \rho_{GT} \overline{\widetilde{U}}_k \overline{\widetilde{U}}_i}{\partial x_k} + \frac{\partial \rho_{GT}\, L_{ki}}{\partial x_k} = -\frac{\partial \rho_{GT} \left(\overline{\widetilde{M}}_{ki} + \overline{\tau}_{ki} \right)}{\partial x_k}. \tag{31}$$

Equation (31) has the same structure as equation (16): the left-hand side describes changes of test-scale velocities (corresponding to the changes of resolved velocities in (16)), and the right-hand side accounts for contributions due to smaller-scale processes.

The methodology applied here to close the equations (30) and (31) is the same as used for the closure of the filtered equations (15) and (16). In analogy to the construction of the stochastic model (17) and (18) in consistency with the equations (15) and (16), a stochastic model that satisfies the equations (30) and (31) is given by

$$\frac{d\widetilde{x}_i^*}{dt} = \widetilde{U}_i^*, \tag{32}$$

$$\frac{d\widetilde{U}_i^*}{dt} = -\frac{1}{\rho_{GT}}\frac{\partial \rho_{GT}\left(\overline{\widetilde{M}}_{ki} + \overline{\tau}_{ki}\right)}{\partial x_k} - \frac{1}{\tau_L^T}\left(\widetilde{U}_i^* - \overline{\widetilde{U}}_i\right) + \sqrt{\frac{4c_0 k^T}{3\tau_L^T}}\frac{dW_i}{dt}. \quad (33)$$

The structure of these equations corresponds to the structure of (17) and (18). A difference is given by the parameters $\tau_L^T = \ell_*^T \Delta^T (k^T)^{-1/2}$ and $k^T = L_{nn}/2$ used here instead of τ_L and k in (18). c_0 is assumed to be unaffected by the scale which appears to be very well justified [12]. A corresponding assumptions is not used with regard to ℓ_*^T due to reasons discussed below.

The consequences of (32) and (33) are very similar to the consequences of (17) and (18). The model (32) and (33) determines a transport equation for the corresponding velocity FDF. The multiplication of this equation with appropriate variables and integration reveals that the model (32) and (33) implies exactly the equations (30) and (31) for the test-filtered mass density and velocities. In correspondence to (20) it is found that the resolved stress L_{ij} satisfies the equation

$$\frac{\overline{\widetilde{D}}L_{ij}}{\overline{\widetilde{D}}t} + \frac{1}{\rho_{GT}}\frac{\partial \rho_{GT} T_{kij}^T}{\partial x_k} + L_{ik}\frac{\partial \overline{\widetilde{U}}_j}{\partial x_k} + L_{jk}\frac{\partial \overline{\widetilde{U}}_i}{\partial x_k} = -\frac{2}{\tau_L^T}\left(L_{ij} - \frac{2}{3}c_0 k^T \delta_{ij}\right). \quad (34)$$

$\overline{\widetilde{D}}/\overline{\widetilde{D}}t = \partial/\partial t + \overline{\widetilde{U}}_k \partial/\partial x_k$ refers to the test-filtered Lagrangian time derivative, and T_{kij}^T is the STS triple correlation tensor of velocity fluctuations. In correspondence to (24), an algebraic model for the deviatoric stress L_{ki}^d is given in the second-order approximation by

$$L_{ij}^d = -2\nu_t^T \overline{\widetilde{S}}_{ij}^d - \nu_t^T \tau_L^T \left[\overline{\widetilde{S}}_{ik}^d \overline{\widetilde{\Omega}}_{kj} + \overline{\widetilde{S}}_{jk}^d \overline{\widetilde{\Omega}}_{ki} - 2\overline{\widetilde{S}}_{ik}^d \overline{\widetilde{S}}_{kj}^d + \frac{2}{3}\overline{\widetilde{S}}_{nk}^d \overline{\widetilde{S}}_{kn}^d \delta_{ij}\right]. \quad (35)$$

The first-order approximation for L_{ki}^d can be obtained by neglecting the nonlinear shear term. $\overline{\widetilde{S}}_{ij}^d$ represents the test-scale deviatoric strain tensor and $\overline{\widetilde{\Omega}}_{ki}$ refers to the test-scale rate-of-rotation tensor. The STS viscosity is defined by $\nu_t^T = k^T \tau_L^T/3$, where $\tau_L^T = \ell_*^T \Delta^T (k^T)^{-1/2}$.

In analogy to expression (25) for the deviatoric SGS stress tensor τ_{ij}^d, expression (35) for the deviatoric resolved stress L_{ki}^d can be written as

$$L_{ij}^d = -c_*^T M_{ij} - c_N^T N_{ij}. \quad (36)$$

Here, the matrices M_{ij} and N_{ij} are given by the expressions

$$M_{ij} = 2\nu_*^T \overline{\widetilde{S}}_{ij}^d, \quad N_{ij} = \left(\Delta^T\right)^2 \left[\overline{\widetilde{S}}_{ik}^d \overline{\widetilde{\Omega}}_{kj} + \overline{\widetilde{S}}_{jk}^d \overline{\widetilde{\Omega}}_{ki} - 2\overline{\widetilde{S}}_{ik}^d \overline{\widetilde{S}}_{kj}^d + \frac{2}{3}\overline{\widetilde{S}}_{nk}^d \overline{\widetilde{S}}_{kn}^d \delta_{ij}\right]. \quad (37)$$

These expressions involve the STS viscosity $\nu_t^T = c_*^T \nu_*^T$. This viscosity ν_t^T can be given either by the non-equilibrium model $c_K^T \nu_K^T$, or it can be given by the equilibrium

model $c_S^T \nu_S^T$,

$$c_*^T \nu_*^T = \left\{ \begin{array}{ll} c_K^T \nu_K^T : & c_K^T = \ell_*^T/3; \quad \nu_K^T = \Delta^T \, (k^T)^{1/2} \\ c_S^T \nu_S^T : & c_S^T = (\ell_*^T/2)^2; \quad \nu_S^T = (\Delta^T)^2 \, |\overline{\overline{S}}^{\, d}| \end{array} \right\}. \tag{38}$$

The parameter c_N^T in (36) is given by $c_N^T = (\ell_*^T)^2/3$. The first-order approximation for L_{ij}^d is recovered by setting $c_N^T = 0$ in (36).

Relation (36) can be used for the dynamic calculation of c_*^T and c_N^T. According to relation (36), the error related to such dynamic estimates for c_*^T and c_N^T is given by $E_{ij} = L_{ij}^d + c_*^T M_{ij} + c_N^T N_{ij}$. The least squares method (i.e. the constraint to minimize the quadratic error $|E|^2$ as a function of c_*^T and c_N^T) then provides for c_*^T, c_N^T, and the related standardized quadratic error $e = |E|^2/|L^d|^2$ the expressions

$$c_*^T = \frac{r_{SN} r_{LN} - r_{LS}}{1 - {r_{SN}}^2} \frac{|L^d|}{2 \nu_*^T |\overline{\overline{S}}^{\, d}|}, \qquad c_N^T = \frac{r_{SN} r_{LS} - r_{LN}}{1 - {r_{SN}}^2} \frac{|L^d|}{|N|},$$

$$e = 1 - \left\{ 1 + \frac{(r_{SN} - r_{LN}/r_{LS})^2}{1 - {r_{SN}}^2} \right\} {r_{LS}}^2. \tag{39}$$

To use relations (39) one has to know how the test-scale coefficients c_K^T, c_S^T, and c_N^T are related to c_K, c_S, and c_N. The definition of these coefficients implies

$$\frac{c_K^T}{c_K} = \frac{\ell_*^T}{\ell_*}, \qquad \frac{c_S^T}{c_S} = \frac{c_N^T}{c_N} = \left(\frac{\ell_*^T}{\ell_*} \right)^2. \tag{40}$$

To evaluate these ratios one has to calculate, therefore, the ratio ℓ_*^T/ℓ_*. By following the development presented in reference [15], one obtains $\ell_*^T/\ell_* = T_\lambda L^T/\Delta^T$. Here, T_λ represents a transfer function and L^T is the characteristic length scale of STS turbulent eddies. The discussion provided in reference [15] reveals that

$$\frac{\ell_*^T}{\ell_*} = \left\{ \begin{array}{ll} 1 & \text{if} \quad \Delta^T \le L^T \\ L^T/\Delta^T & \text{if} \quad \Delta^T \ge L^T \end{array} \right\}. \tag{41}$$

Hence, the test-scale coefficients c_K^T, c_S^T, and c_N^T represent very good estimates for c_K, c_S, and c_N provided that $\Delta^T \le L^T$. The latter condition will be considered to be given in the following.

By adopting $c_*^T = c_*$ and $c_N^T = c_N$ in relations (39), c_*, c_N, and the standardized error are given by

$$c_* = \frac{r_{SN} r_{LN} - r_{LS}}{1 - {r_{SN}}^2} \frac{|L^d|}{2 \nu_*^T |\overline{\overline{S}}^{\, d}|}, \qquad c_N = \frac{r_{SN} r_{LS} - r_{LN}}{1 - {r_{SN}}^2} \frac{|L^d|}{|N|},$$

$$e_{\mathrm{NDM}} = 1 - \left\{ 1 + \frac{(r_{SN} - r_{LN}/r_{LS})^2}{1 - {r_{SN}}^2} \right\} {r_{LS}}^2. \tag{42}$$

The calculation of model coefficients in (25) according to (42) will be referred to as nonlinear dynamic model (NDM). Relation (42) can be simplified by neglecting the nonlinear term N_{ij} in (36). The latter assumption results in the following expressions for c_*, c_N, and the standardized error,

$$c_* = -\frac{r_{LS}}{2} \frac{|L^d|}{\nu_*^T |\widetilde{\overline{S}}^d|}, \qquad c_N = 0, \qquad e_{\mathrm{LDM}} = 1 - {r_{LS}}^2. \tag{43}$$

The calculation of model coefficients in (25) according to (43) will be referred to as linear dynamic model (LDM).

6. Comparisons with other dynamic SGS stress models

Next, let us compare the LDM and the NDM derived in Section 5 with corresponding other SGS stress models. These comparisons will be performed in the following way. First, the $c_*\nu_* = c_S\nu_S$ version of the LDM will be compared to the DSM. The structure of both models is equal. The only difference is given by the dynamic procedure to calculate the Smagorinsky coefficient c_S. Second, the $c_*\nu_* = c_K\nu_K$ version of the LDM will be compared to Kim and Menon's localized dynamic k-equation model (LDKM) [18, 19]. Both models are equal if a dynamic calculation of the SGS dissipation rate is added to the $c_*\nu_* = c_K\nu_K$ version of the LDM. Nevertheless, there are differences regarding the theoretical support for the LDKM and LDM. Third, both versions of the LDM will be compared to the NDM to see the relevance of involving nonlinear shear contributions.

The comparison between the $c_*\nu_* = c_S\nu_S$ version of the LDM with the DSM described and analyzed in Sections 2 and 3, respectively, shows that the DSM concept is not in consistency with the realizability constraint discussed in Section 1, whereas the LDM is realizable. Which consequences does this finding imply for the performance of these models? To address this question, let us consider the DSM error e_S in comparison to the LDM error $e_{\mathrm{LDM}} = 1 - {r_{LS}}^2$. According to expression (8), e_S depends on r_{LS} and (via Δ_{LR} and Δ_{SR}) on γr^2 and the parameters r_{LS}, r_{LR}, and r_{SR}. To reduce this complex dependence, it is helpful to simplify Δ_{LR} and Δ_{SR} which vanish if the approximation $R_{ij} = \widetilde{\overline{S}}^d_{ij}$ is used (see Section 3). For doing this, we use the first-order approximation $L^d_{ij} = -2\nu_t^T \widetilde{\overline{S}}^d_{ij}$ for the resolved stress tensor which is implied by the stochastic model (17) and (18). The latter assumption implies $r_{LR} = -r_{SR}$ and $r_{LS} = -1$. Accordingly, Δ_{SR} is unchanged, but Δ_{LR} is now given by $\Delta_{LR} = (1 - r_{SR})\gamma r^2/(1 - \gamma r^2)$. The resulting DSM error e_S reads

$$e_S = 1 - \frac{\left(r_{LS}(1 - \gamma r^2) - (1 - r_{SR})\gamma r^2\right)^2}{(1 - \gamma r^2)^2 - 2(r_{SR} - 1)\gamma r^2}. \tag{44}$$

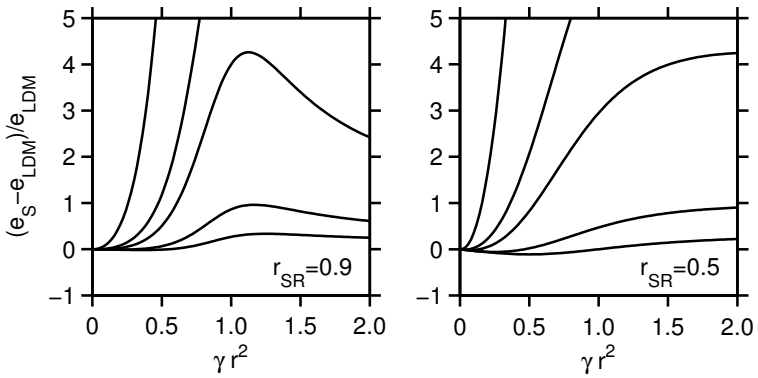

Figure 1. The normalized error difference $(e_S - e_{\text{LDM}})/e_{\text{LDM}}$ between the DSM error e_S and LDM error e_{LDM}. Here, $r = \Delta/\Delta^T$ and $\gamma = |R|/|\overline{\overline{S}}^d|$. The left hand side shows the case $r_{SR} = 0.9$, and the right-hand side shows the case $r_{SR} = 0.5$. In both figures, curves are shown for $r_{LS} = -0.5$, $r_{LS} = -0.7$, $r_{LS} = -0.9$, $r_{LS} = -0.95$ and $r_{LS} = -0.99$. The curve with the lowest peak value is found for $r_{LS} = -0.5$, and the curve with the highest peak value is found for $r_{LS} = -0.99$.

The complex dependence of expression (8) is reduced in this way because e_S depends now only on the parameters r_{LS} and r_{SR}. One can show that $e_S \geq 0$ provided that $r_{LS} \leq r_{SR}$. A convenient way to analyze the difference between the DSM error e_S given by (44) and LDM error $e_{\text{LDM}} = 1 - {r_{LS}}^2$ is to consider the relative error $(e_S - e_{\text{LDM}})/e_{\text{LDM}}$. An illustration of this error $(e_S - e_{\text{LDM}})/e_{\text{LDM}}$ in dependence on γr^2 is given in Figure 1. Guideline for the range of r_{LS} values that should be considered can be obtained by taking again reference to the first-order approximation $L^d_{ij} = -2\nu_t^T \overline{\overline{S}}^d_{ij}$ for L^d_{ij}, which implies that $r_{LS} = -1$. Correspondingly, a range $-0.99 \leq r_{LS} \leq -0.5$ was applied in Figure 1. With regard to r_{SR}, two values $r_{SR} = 0.9$ and $r_{SR} = 0.5$ were considered to characterize the effect of r_{SR} variations in a range $r_{SR} \leq 1$ (the value $r_{SR} = 1$ corresponds to the approximation $R_{ij} = \overline{\overline{S}}^d_{ij}$). The illustration in Figure 1 shows that the minimum of the relative error is close to zero, but the maximum relative error may be significantly larger than zero (which means that the DSM error e_S can be much larger than the LDM error e_{LDM}). The minimum and maximum values of the curves shown in Figure 1 can be found by analyzing $(e_S - e_{\text{LDM}})/e_{\text{LDM}}$ as a function of γr^2 (a maximum is found if the condition $1 + r_{LS} \leq r_{SR}$ is satisfied). This analysis reveals that a minimum of $(e_S - e_{\text{LDM}})/e_{\text{LDM}}$ is given at $\gamma r^2 = (1 + r_{LS})/(r_{SR} - r_{LS})$, and a maximum is given at $\gamma r^2 = r_{LS}/(1 + r_{LS} - r_{SR})$. Hence, the relative error $(e_S - e_{\text{LDM}})/e_{\text{LDM}}$ is found to be bounded according to

$$-\frac{(1 - r_{SR})\,(1 + r_{LS})}{(1 + r_{SR})\,(1 - r_{LS})} \leq \frac{e_S - e_{\text{LDM}}}{e_{\text{LDM}}} \leq \frac{{r_{LS}}^2}{1 - {r_{LS}}^2}. \tag{45}$$

By considering relation (45) for the case $r_{LS} \to -1$ one finds that the minimum of $(e_S - e_{\mathrm{LDM}})/e_{\mathrm{LDM}}$ goes to zero and the maximum goes to infinity. Such possibly huge errors may well support the development of instabilities and physically incorrect solutions. The use of the realizable LDM enables, therefore, more stable simulations compared to the non-realizable DSM. It is worth noting that the reason for the disadvantages of the DSM is given by the scale dependence of the DSM via $r = \Delta/\Delta^T$, which implies a variation of c_S with r that is driven by a divergence.

The comparison between the $c_*\nu_* = c_K\nu_K$ version of the LDM with Kim and Menon's LDKM [18, 19] shows that the LDM agrees with the LDKM if a dynamic calculation of the SGS dissipation rate is added. Therefore, the LDKM also represents a realizable SGS stress model. What is the advantage of the development presented here compared to the introduction of the LDKM? The LDKM was introduced by referring to the scale similarity $\tau_{ij} = \kappa L_{ij}$ observed in measurements, where the resolved stress is given here by its definition $L_{ki} = \widetilde{\widetilde{U}_k\widetilde{U}_i} - \widetilde{\widetilde{U}}_k\widetilde{\widetilde{U}}_i$ and $\kappa = 0.45 \pm 0.15$ [24]. Based on this observation Kim and Menon [18, 19] concluded that $L^d_{ij} = -2c^T_K\nu^T_K\,\widetilde{\widetilde{S}}^{\,d}_{ij}$, which was used for the dynamic calculation of $c_K = c^T_K$. However, the similarity in variation $\tau_{ij} = \kappa L_{ij}$ for τ_{ij} and L_{ij} does not imply the LDKM assumption $L^d_{ij} = -2c^T_K\nu^T_K\,\widetilde{\widetilde{S}}^{\,d}_{ij}$ (the latter conclusion is just a plausible assumption which may be correct or not). Hence, the LDKM assumption for L^d_{ij} was obtained without significant theoretical support. The latter is not the case regarding the LDM which was obtained here as the result of a systematic development of realizable SGS stress models. In addition to the consistency with the LDKM, the derivation of the LDM also provides an attractive alternative: the $c_*\nu_* = c_S\nu_S$ version of the LDM which is related to lower computational costs (because there is no need to solve a transport equation for the residual turbulent kinetic energy). Regardless the theoretical development, the fact that the LDKM was successfully applied to several cases [18, 19] further supports the validity of the LDM concept.

The comparison between the LDM with the NDM reveals the advantage of realizable nonlinear dynamic stress models. One may expect that nonlinear models are advantageous, in particular for complex flow simulations. Explicit evidence for this view is obtained by comparing the NDM with the LDM: one observes that the NDM error is smaller than the LDM error: see (42) and (43).

7. Summary

Stochastic analysis was already shown to represent a powerful tool for the derivation of realizable linear and nonlinear SGS stress models [11, 12, 14], and for the development of unified turbulence models that can be used continuously as LES and RANS, or FDF and PDF methods [15]. Here, it was shown that stochastic analysis is also very helpful for the development of realizable linear and nonlinear dynamic SGS stress models.

The specific results obtained by the stochastic analysis applied are the following ones. First, the realizable LDM has theoretical and practical advantages compared to the non-realizable DSM: the LDM does not involve an incorrect scale dependence which avoids the appearance of errors that can be significantly larger than the LDM errors. The possibly huge errors of the DSM may support the development of instabilities and physically incorrect solutions. Second, the realizable LDM also has theoretical and practical advantages compared to the LDKM: the LDM is the result of a well based systematic development of realizable SGS stress models, and it offers the $c_*\nu_* = c_S\nu_S$ version of the LDM as an attractive alternative. Regarding the differences between both LDM versions it is worth emphasizing that the error $e_{\mathrm{LDM}} = 1 - {r_{LS}}^2$ of both versions is the same, but the $c_*\nu_* = c_S\nu_S$ version of the LDM is related to lower computational costs because there is no need to solve a transport equation for the residual turbulent kinetic energy. Third, the realizable NDM represents a valuable alternative to the LDM: it reduces the error of computations in such a way that the computational costs are hardly increased by the inclusion of nonlinear shear contributions [48].

Acknowledgments. This work was supported in part by the U.S. Air Force Office of Scientific Research (Grant No. DODAF41603). Dr. John Schmisseur is the Program Manager for this grant.

References

1. P. A. Durbin and B. A. Petterson, *Statistical Theory and Modeling for Turbulent Flows*, John Wiley and Sons, Chichester, New York, Weinheim, Brisbane, Singapore, Toronto, 2001.
2. P. A. Durbin and C. G. Speziale, Realizability of second-moment closure via stochastic analysis, *Journal of Fluid Mechanics* **280** (1994), pp. 395–407.
3. R. O. Fox, *Computational Models for Turbulent Reacting Flows*, Cambridge University Press, Cambridge, UK, 2003.
4. C. Fureby and G. Tabor, Mathematical and physical constraints on large-eddy simulations, *Theoretical and Computational Fluid Dynamics* **9** (1997), pp. 85–102.
5. M. Germano, Fundamentals of large eddy simulation, in: *Advanced Turbulent Flows Computations. CISM Courses and Lectures 395* (R. Peyret and E. Krause, eds.), pp. 81–130, Springer, Berlin, Heidelberg, New York, 2000.
6. M. Germano, U. Piomelli, P. Moin and W. H. Cabot, A dynamic subgrid-scale eddy viscosity model, *Physics of Fluids A* **3** (1991), pp. 1760–1765.
7. S. Ghosal, Mathematical and physical constraints on large-eddy simulation of turbulence, *AIAA Journal* **37** (1999), pp. 425–433.
8. L. Y. M. Gicquel, P. Givi, F. A. Jaberi and S. B. Pope, Velocity filtered density function for large eddy simulation of turbulent flows, *Physics of Fluids* **14** (2002), pp. 1196–1213.
9. S. S. Girimaji, A new perspective on realizability of turbulence models, *Journal of Fluid Mechanics* **512** (2004), pp. 191–210.

10. P. Givi, Filtered density function for subgrid scale modeling of turbulent combustion, *AIAA Journal* **44** (2006), pp. 16–23.

11. S. Heinz, On Fokker-Planck equations for turbulent reacting flows. Part 2. Filter density function for large eddy simulation, *Flow, Turbulence and Combustion* **70** (2003), pp. 153–181.

12. _____, *Statistical Mechanics of Turbulent Flows*, Springer, Berlin, Heidelberg, New York, 2003.

13. _____, Molecular to fluid dynamics: The consequences of stochastic molecular motion, *Physical Review E* **70** (2004), pp. 036308/1–11.

14. _____, Comment on "A dynamic nonlinear subgrid-scale stress model" [Phys. Fluid 17, 035109 (2005)], *Physics of Fluids* **17** (2005), pp. 099101/1–2.

15. _____, Unified turbulence models for LES and RANS, FDF and PDF simulations, *Theoretical and Computational Fluid Dynamics* **21** (2007), pp. 99–118.

16. K. Horiuti, Roles of non-aligned eigenvectors of strain-rate and subgrid-scale stress tensors in turbulence generation, *Journal of Fluid Mechanics* **491** (2003), pp. 65–100.

17. A. V. Johansson and M. Hallback, Modelling of rapid pressure-strain in Reynolds stress closures, *Journal of Fluid Mechanics* **269** (1994), pp. 143–168.

18. W.-W. Kim, *A new dynamic subgrid-scale model for large-eddy simulation of turbulent flows*, Ph.D. thesis, School of Aerospace Engineering, Georgia Institute of Technology, Atlanta, Georgia, 1996.

19. W.-W. Kim and S. Menon, Application of the localized dynamic subgrid-scale model to turbulent wall-bounded flows, *AIAA Paper* **97-0210** (1997).

20. B. Kosović, Subgrid-scale modeling for the large eddy simulation of high-Reynolds number boundary layers, *Journal of Fluid Mechanics* **336** (1997), pp. 151–182.

21. M. Lesieur, O. Métais and P. Comte, *Large-Eddy Simulations of Turbulence*, Cambridge University Press, Cambridge, UK, 2005.

22. D. K. Lilly, The representation of small-scale turbulence in numerical simulation of experiments, in: *Proceedings of the IBM Scientific Computing Symposium on Environmental Sciences* (H. H. Goldstine, ed.), pp. 195–210, IBM, Yorktown Heights, NY, 1967.

23. _____, A proposed modification of the Germano subgrid-scale closure method, *Physics of Fluids A* **4** (1992), pp. 633–635.

24. S. Liu, C. Meneveau and J. Katz, On the properties of similarity subgrid-scale models as deduced from measurements in a turbulent jet, *Journal of Fluid Mechanics* **275** (1994), pp. 83–119.

25. J. L. Lumley, Computational modeling of turbulent flows, *Advances in Applied Mechanics* **18** (1978), pp. 123–175.

26. L. Marstorp, G. Brethouwer and A. V. Johansson, A stochastic subgrid model with application to turbulent flow and scalar mixing, *Physics of Fluids* **19** (2007), pp. 035107/1–12.

27. C. Meneveau and J. Katz, Dynamic testing of subgrid models in large eddy simulation based on the Germano identity, *Physics of Fluids* **11** (1999), pp. 245–247.

28. _____, Scale-invariance and turbulence models for large eddy simulation, *Annual Review of Fluid Mechanics* **32** (2000), pp. 1–32.

29. C. Meneveau, T. S. Lund and W. H. Cabot, A Lagrangian dynamic subgrid-scale model for turbulence, *Journal of Fluid Mechanics* **319** (1996), pp. 353–385.

30. B. Merci, C. De Langhe and J. Vierendeels, A quasi-realizable cubic low-Reynolds eddy-viscosity turbulence model with a new dissipation rate equation, *Flow, Turbulence and Combustion* **66** (2001), pp. 133–157.

31. M. Muradoglu, P. Jenny, S. B. Pope and D. A. Caughey, A consistent hybrid finite-volume/particle method for the PDF equations of turbulent reactive flows, *Journal of Computational Physics* **154** (1999), pp. 342–371.

32. P. A. Nooren, H. A. Wouters, T. W. J. Peeters and D. Roekaerts, Monte Carlo PDF modeling of a turbulent natural-gas diffusion flame, *Combustion Theory and Modeling* **1** (1997), pp. 79–96.

33. U. Piomelli, Large eddy simulation: Achievements and challenges, *Progress in Aerospace Sciences* **35** (1999), pp. 335–362.

34. H. Pitsch, Large eddy simulation of turbulent combustion, *Annual Review of Fluid Mechanics* **38** (2006), pp. 453–482.

35. S. B. Pope, PDF methods for turbulent reactive flows, *Progress in Energy and Combustion Science* **11** (1985), pp. 119–192.

36. _____, On the relationship between stochastic Lagrangian models of turbulence and second-moment closures, *Physics of Fluids* **6** (1994), pp. 973–985.

37. _____, *Turbulent Flows*, Cambridge University Press, Cambridge, UK, 2000.

38. V. Raman, H. Pitsch and R. O. Fox, Hybrid large eddy simulation/Lagrangian filtered-density-function approach for simulating turbulent combustion, *Combustion and Flame* **143** (2005), pp. 56–78.

39. J. R. Ristorcelli, J. L. Lumley and R. Abid, A rapid-pressure covariance representation consistent with the Taylor-Proudman theorem materially frame indifferent in the two-dimensional limit, *Journal of Fluid Mechanics* **292** (1995), pp. 111–152.

40. S. Sagaut, *Large Eddy Simulation for Incompressible Flows*, Springer, Berlin, Heidelberg, New York, 2005.

41. U. Schumann, Realizability of Reynolds stress turbulence models, *Physics of Fluids* **20** (1977), pp. 721–725.

42. M. R. H. Sheikhi, T. G. Drozda, P. Givi, F. A. Jaberi and S. B. Pope, Large eddy simulation of a turbulent nonpremixed piloted methane jet flame (Sandia Flame D), *Proceedings of the Combustion Institute* **30** (2005), pp. 549–556.

43. M. R. H. Sheikhi, T. G. Drozda, P. Givi and S. B. Pope, Velocity-scalar filtered density function for large eddy simulation of turbulent flows, *Physics of Fluids* **15** (2003), pp. 2321–2337.

44. T. Sjögren and A. V. Johansson, Development and calibration of algebraic nonlinear models for terms in the Reynolds stress transport equations, *Physics of Fluids* **12** (2000), pp. 1554–1572.

45. C. G. Speziale, R. Abid and P. A. Durbin, New results on the realizability of Reynolds stress turbulence closures, *ICASE Report* **93-76** (1993), pp. 1–47.

46. R. Du Vachat, Realizability inequalities in turbulent flows, *Physics of Fluids* **20** (1977), pp. 551–556.

47. B. Vreman, B. Geurts and H. Kuerten, Realizability conditions for the turbulent stress tensor in large-eddy simulation, *Journal of Fluid Mechanics* **278** (1994), pp. 351–362.

48. B. C. Wang and D. J. Bergstrom, A dynamic nonlinear subgrid-scale stress model, *Physics of Fluids* **17** (2005), pp. 035109/1–15.

49. V. C. Wong, A proposed statistical-dynamic closure method for the linear or nonlinear subgrid-scale stresses, *Physics of Fluids A* **4** (1992), pp. 1080–1082.

50. H. A. Wouters, P. A. Nooren, T. W. J. Peeters and D. Roekaerts, Simulation of a bluff-body stabilized diffusion flame using second-moment closure and Monte Carlo methods, *Proceedings of the Combustion Institute* **26** (1996), pp. 177–185.

51. H. A. Wouters, T. W. J. Peeters and D. Roekaerts, On the existence of a generalized Langevin model representation for second-moment closures, *Physics of Fluids* **8** (1996), pp. 1702–1704.

Received May 10, 2008; revised October 02, 2008

Author information

Stefan Heinz, Department of Mathematics, University of Wyoming, 1000 East University Avenue, Laramie, WY 82071, USA.
Email: heinz@uwyo.edu